ISSN 1061-933X, Colloid Journal, 2017, Vol. 79, No. 2, pp. 181–189. © Pleiades Publishing, Ltd., 2017.
Original Russian Text © N.A. Volkov, N.V. Tuzov, A.K. Shchekin, 2017, published in Kolloidnyi Zhurnal, 2017, Vol. 79, No. 2, pp. 124–133.

All-Atom Molecular Dynamics Analysis of Kinetic and Structural Properties of Ionic Micellar Solutions

N. A. Volkov, N. V. Tuzov, and A. K. Shchekin*

St. Petersburg State University, Universitetskaya nab. 7/9, St. Petersburg, 199034 Russia

**e-mail: a.shchekin@spbu.ru*

Received August 19, 2016

Abstract—All-atom molecular dynamics simulation results regarding aqueous sodium dodecyl sulfate (SDS) solutions have been presented. Both salt-free solutions with different SDS concentrations and those containing calcium chloride additives have been studied. The simulation has shown that surface-active SDS ions form stable premicellar aggregates. The obtained molecular dynamics trajectories have been used to describe both the kinetic and structural properties of solutions containing SDS molecular aggregates and the properties of individual aggregates. Aggregation kinetics has been investigated, and the characteristic sizes of the aggregates have been calculated by different methods. It has been found that the size of a premicellar aggregate with aggregation number $n = 16$ in a salt-free solution virtually does not depend on surfactant concentration. Radial distribution functions (RDFs) of hydrogen and oxygen atoms of water molecules relative to the center of mass of an aggregate have no local maxima near the aggregate surface; i.e., the surface is incompletely wetted with water. Corresponding RDFs of carbon atoms have one, two or three maxima depending on the surfactant concentration and the serial number of a carbon atom in the hydrocarbon radical of the surface-active ion. The study of the potentials of mean force for the interaction of sodium and calcium ions with an aggregate having aggregation number $n = 32$ shows that only calcium ions can be strongly bound to such an aggregate.

DOI: 10.1134/S1061933X17020156

INTRODUCTION

The dynamics of aggregation and aggregate disruption in micellar solutions may be theoretically described by fundamental kinetic equations, such as the Becker–Döring equation or the generalized Smoluchowski equation [1–6]. In these equations, the coefficients of attachment–detachment of monomers or aggregates depend on the diffusion coefficients of micelles, premicellar aggregates, surface-active ions, counterions, and coions, as well as the degree of micelle-surface coverage with polar groups [6, 7]. Thus, kinetic phenomena in micellar solutions strongly depend on their diffusion and structural features caused by the presence of molecular aggregates.

It is known that real micellar solutions contain aggregates with different aggregation numbers. These aggregates are very difficult to distinguish and, hence, study separately even with the use of modern experimental equipment and procedures. This is the case for, e.g., studies performed using such methods as dynamic light scattering and nuclear-magnetic resonance. At the same time, the methods of molecular simulation allow one to study in detail the transport and structural properties of separate aggregates with arbitrary aggregation numbers within the frameworks of mathematical experiments.

Different groups of researchers have successfully used molecular dynamics simulations to study micellar solutions of both ionic and nonionic surfactants (see reviews [8–10]). Therewith, the all-atom model of a surfactant and a solvent has commonly been used to simulate a system containing a single preliminarily assembled micelle with an aggregation number characteristic for the surfactant under consideration and corresponding to the large stable micelle. At the same time, the properties of premicellar aggregates, which are inevitably present in micellar solutions, as well as the aggregation kinetics of individual aggregates, have scarcely been considered. In [11, 12], the self-aggregation of surface-active ions in aqueous sodium dodecyl sulfate (SDS) solutions, including those containing additives of a 1 : 1 electrolyte, was simulated, and the transport and structural properties of the formed premicellar aggregates were studied by the all-atom molecular dynamics method. Micellization in a salt-free SDS solution and solutions containing NaCl and $CaCl_2$ was studied in [13, 14] by molecular dynamics within the framework of the united-atom model. In [15], all-atom molecular dynamics was used to study micellization kinetics at short times in solutions of ionic and nonionic surfactants.

Table 1. Partial charges for an SDS molecule (in elementary charge units): Na^+ is the sodium ion, S is the sulfur atom, OS_1 is the oxygen atom between S and first carbon atom C_1, OS_{2-4} denotes three other O atoms located next to S, and C_{1-12} denotes 12 C atoms in the hydrocarbon radical (their serial numbers are counted in the hydrocarbon radical beginning from the head group)

Atom	Charge	Atom	Charge
Na^+	+1.0	C_1	–0.28
S	+1.33	C_{2-11}	–0.18
OS_1	–0.28	C_{12}	–0.27
OS_{2-4}	–0.65	H	+0.09

It is of substantial interest to use all-atom molecular dynamics for studying the equilibrium properties of micellar systems with large numbers of surfactant molecules. At corresponding surfactant concentrations, these systems contain free surface-active monomers, short-lived premicellar aggregates with different aggregation numbers (dimers, trimers, etc.), and relatively stable micelles. The study of systems containing large numbers of surfactant molecules in all-atom representation leads to the consumption of large computational and time resources. However, even small micellar systems containing one or two aggregates, which appear to be quasi-stable in simulation cells of rather small size, may be used to study the transport and structural properties of these aggregates. For example, the minimum cell size and simulation time necessary to determine the structural properties of a micellar solution may be found by analyzing the aggregation kinetics of individual aggregates and by studying the form and stability of different radial distribution functions (RDFs). RDFs with rather smooth and expected patterns (having characteristic local maxima, minima, and asymptotics at large distances) will indicate that a system has reached, at least, mechanical and thermal equilibrium.

In this work, all-atom molecular dynamics method has been used to study micellization kinetics in an aqueous solution of SDS ($C_{12}H_{25}NaSO_4$) beginning from the configuration, in which the surface-active ions are uniformly distributed in a simulation cell. The simulation has shown the formation of short-lived aggregates consisting of a few monomers followed by their coalescence into larger relatively stable aggregates, which, in the long run, comprise all surface-active ions present in the cell, but, however, appear to be smaller than stable micelles in an infinite solution at the same total concentration of the surfactant. Analysis of molecular dynamics trajectories is employed to describe the kinetic and structural properties of a micellar solution containing formed premicellar aggregates, as well as the properties of the aggregates themselves. Both salt-free aqueous SDS solutions and those containing $CaCl_2$ have been considered.

1. MICELLAR-SOLUTION MODEL AND CALCULATION METHOD

Molecular dynamics simulation was performed using the MDynaMix v.5.2.7 software package [16] and the CHARMM36 classical force field [17]. In addition, we developed a number of in-house computer programs for the analysis of molecular dynamics trajectories. In the classical molecular dynamics simulation, atoms are provided with partial charges, which remain unchanged throughout the modeling. Table 1 lists the partial charges for an SDS molecule taken from the "CHARMM36 All-Hydrogen Lipid Topology File" available on the official website of the developers of the CHARMM force field [18].

We used the following atomic weights, charges, and Lennard-Jones (LJ) potential parameters [19] for sodium, calcium, and chlorine ions [20]: $M_{Na^+} = 22.9898$ amu, $q_{Na^+} = e$ (one elementary charge), $\sigma_{Na^+} = 2.8215$ Å, and $\varepsilon_{Na^+} = 0.196$ kJ/mol; $M_{Ca^{2+}} = 40.08$ amu, $q_{Ca^{2+}} = 2e$, $\sigma_{Ca^{2+}} = 2.734$ Å, and $\varepsilon_{Ca^{2+}} = 0.502$ kJ/mol; and $M_{Cl^-} = 35.45$ amu, $q_{Cl^-} = -e$, $\sigma_{Cl^-} = 4.54$ Å, and $\varepsilon_{Cl^-} = 0.6276$ kJ/mol. The parameters were taken from the official website of the developers of the CHARMM force field [18].

For water, we, as in [11, 12], have used the CHARMM TIP3P model, i.e., the so-called "TIPS3P model" [21–23], which is a modification of the TIP3P model [24]. In contrast to the TIP3P model, the TIPS3P model implies a nonzero LJ potential for hydrogen atoms. We used the following LJ parameters for them: $\sigma = 0.4$ Å, and $\varepsilon = 0.192$ kJ/mol.

The simulation was performed in the *NPT* ensemble using a cubic simulation cell with periodic boundary conditions. The temperature and pressure were controlled using the Nosé thermostat with temperature $T = 298$ K and the Nosé–Hoover barostate with a target pressure of 1 atm. Instead of imposing limitations on the lengths of interatomic bonds, a double-time-step algorithm [25] was used with short and long steps of 0.2 and 2 fs, respectively. The translational motion of the center of mass of the system was eliminated every 200 fs. The Ewald method [26] was used to take into account electrostatic interactions. The cutoff radius for LJ interactions, which were calculated at each short step, was 5 Å. The LJ potentials calculated at each long step and the Ewald sum component calculated in real space were cut off at distance $R_{cut} = 12$ Å. In addition to cutoff radius R_{cut} in the real space, the calculation accuracy of the Ewald sum is affected by two more parameters, i.e., the cutoff radius in the Fourier space and the so-called convergence parameter. In the MDynaMix software package, the calculation accuracy of the Ewald sum is preset by special constants B and A. The calculation accu-

racy of the Ewald sum component in the real space is determined by the value of complementary error function erfc(A). Constant B specifies the cutoff radius of the Ewald sum component calculated in the Fourier space, with the calculation accuracy of this component being exp($-B$). We used values $A = 2.8$ and $B = 9$, which are specified in the MDynaMix package by default [27].

Preliminarily, we studied several systems with different sizes and compositions; the parameters of these systems are presented in Table 2. The considered systems contained 16 or 32 surfactant molecules. The numbers of TIPS3P water molecules per SDS molecule were, in the case of the salt-free solution, 200, 300, and 400; for the salt-containing solution, it was 100. As a result, the systems contained 3200, 4800, or 6400 water molecules. Simulation time t_{sim} was varied from 74 to 109 ns, depending on the system size. In all the considered cases, all surface-active ions gathered into a single aggregate in 10–30 ns. This aggregate retained its aggregation number until the end of the simulation. The averages were calculated from the moment of aggregate formation until the end of the simulation. The following structural properties were studied for these stable aggregates: different RDFs and characteristic size.

The all-atom molecular dynamics of micellar solutions is much more laborious than the molecular dynamics using coarse-grained models. The all-atom simulation of a micellar ensemble composed of several hundreds or, at least, a few tens of aggregates (which is necessary for determining distributions over aggregation numbers) and a reasonable number of solvent molecules would require significant computational resources, especially when both equilibrium and dynamic properties are to be studied. As has been mentioned above, simulation is often implemented by considering a cell containing a single aggregate preliminarily assembled from surface-active ions. This approach enables one to reduce the simulation time; however, the aggregation number must be preliminarily specified in this case.

No preliminarily assembled aggregates were used in our simulation. Initially, all SDS molecules were randomly oriented and uniformly distributed throughout the simulation cell in a manner such that their centers formed a face-centered cubic lattice. At early stages of the simulation, small aggregates were formed and gradually fused into larger aggregates, which remained unchanged for several tens of nanoseconds. Of course, this time was too short to equilibrate a micellar solution; nevertheless, it was sufficient for statistics gathering and obtaining reliable data on the structural properties of the micellar solution.

In addition to the salt-free systems, a system containing a 2 : 1 electrolyte ($CaCl_2$) was simulated. The number of added salt molecules was half the number of surfactant molecules. For the salt-free micellar solutions, several surfactant concentrations were considered. At the same time, the number of SDS molecules in the cell was constant, $N_{SDS} = 16$, while the number of water molecules varied: $N_{H_2O} = 3200$, 4800, and 6400.

Table 2. Parameters of studied systems: N_{SDS}, N_{H_2O}, and N_{CaCl_2} are the numbers of surfactant, H_2O, and $CaCl_2$ molecules in the simulation cell, respectively, and t_{sim} is the simulation time

N_{SDS}	N_{H_2O}	N_{CaCl_2}	t_{sim}, ns
16	3200	–	101
16	4800	–	105
16	6400	–	109
32	3200	16	74

2. RESULTS

The coordinates of the aggregate centers of mass (CMs) were determined by analyzing molecular dynamics trajectories in order to plot the RDFs of atoms and ions relative to the CM coordinates. The CMs were calculated by the following formula:

$$\vec{C}_m = \frac{\sum_{i=1}^{N} m_i \vec{q}_i}{M}, \quad (1)$$

where m_i is the mass of an ith atom, $\vec{q}_i$ denotes the radius-vector of the ith atom, and $M = \sum_{i=1}^{N} m_i$. Therewith, when calculating the CM of an aggregate, only atoms belonging to the surface-active ions were taken into account, N is the total number of such atoms.

In some cases, an aggregate appeared to be divided by the boundaries of the periodic cell (see, e.g., Fig. 1). In this situation, its CM was determined using a special procedure [11]. Shifting all surface-active ions along the OX, OY, and OZ coordinate axes and remembering the shift values, we placed the entire aggregate into the cell center. The CM coordinates were determined for this continuous aggregate by formula (1). The position of the CM for the initial aggregate was found taking into account the shifts that had been performed along the OX, OY, and OZ axes. The result of this procedure, as applied to the aggregate depicted in Fig. 1, is presented in Fig. 2.

Having determined the position of the aggregate CM, we may find the characteristic size R_S of the aggregate by the following formula proposed in [28]:

$$R_S = \sqrt{\frac{5}{3}} R_g, \quad (2)$$

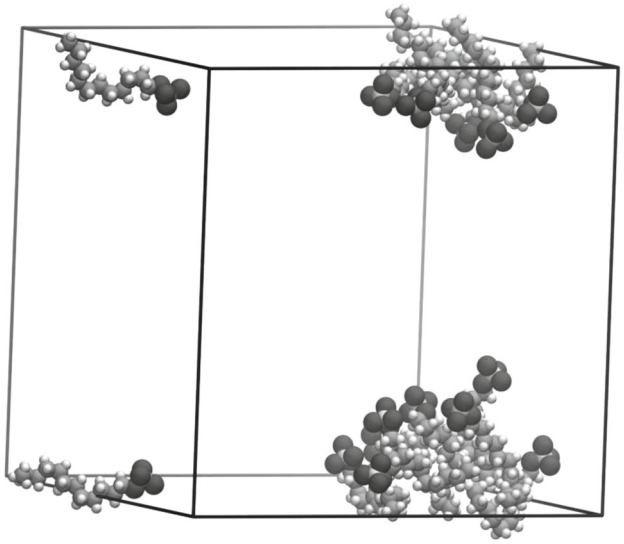

Fig. 1. A snapshot of the simulation cell containing 16 surface-active ions (water molecules and counterions are not shown). In this case, the aggregate is divided by the boundaries of the periodic cell.

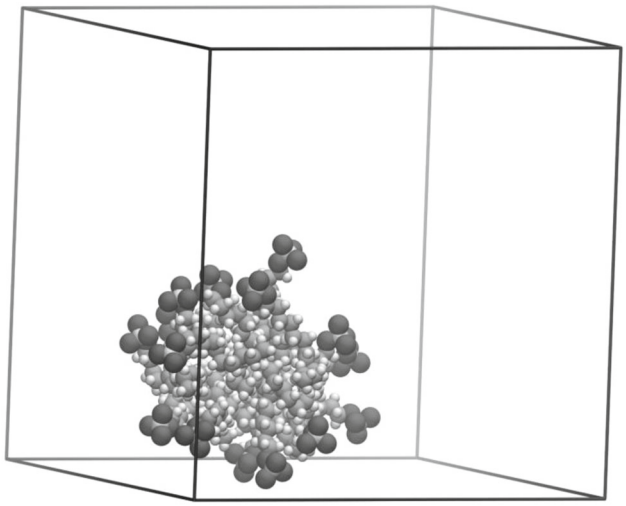

Fig. 2. An aggregate (Fig. 1) subjected to parallel shifts.

where R_g is the average gyration radius for the aggregate,

$$R_g = \sqrt{\frac{1}{N}\sum_{i=1}^{N} r_i^2}; \quad (3)$$

N is the total number of atoms in the aggregate; and r_i is the distance from the ith atom to the aggregate CM. Formula (2) represents the relation between the radius and the gyration radius for a solid sphere with a constant density; nevertheless, it may be used to determine the size of a micelle. In the case of the salt-free solution, the sizes calculated by expression (2) for aggregates composed of 16 surface-active ions in systems containing 3200, 4800, and 6400 water molecules appeared to be almost equal: R_S = 12.3 Å. The error was no larger than 0.2 Å. Thus, it may be stated that the size of the examined premicellar aggregate with aggregation number $n = 16$ is almost independent of surfactant concentration within the studied concentration range.

Figures 3–7 show the $g(r)$ RDFs (r is the distance from an ion or atom to the aggregate CM) for the following systems: one aggregate with aggregation number $n = 16$ and the numbers of water molecules N_{H_2O} = 3200, 4800, and 6400 in a salt-free SDS solution and (Figs. 3–4 only) one aggregate with aggregation number $n = 32$ and the number of water molecules N_{H_2O} = 3200 in an SDS solution in the presence of 16 $CaCl_2$ molecules. The following normalization was used for the $g(r)$ RDFs: $\int 4\pi g(r) r^2 dr = V$, where V is the average volume of the simulation cell (in the *NPT* ensemble, the edge length and volume of the cubic cell fluctuate about their equilibrium values); the integration was performed from zero to R_{max}, which is the minimum half-length of the cubic cell edge realized in the simulation.

Let us consider the behavior of the RDFs relative to the aggregate CM for sodium ions and sulfur atoms (Figs. 3 and 4). The vertical lines in Fig. 4 correspond to R_S values (formula (2)). Figure 4 shows that the positions of RDF maxima for sulfur atoms are close to the values of effective aggregate sizes R_S, as we previously observed for other systems [12]. The RDF curves for sodium ions relative to the CM of an aggregate with aggregation number $n = 16$ at different overall surfactant concentrations have the similar pattern (Fig. 3).

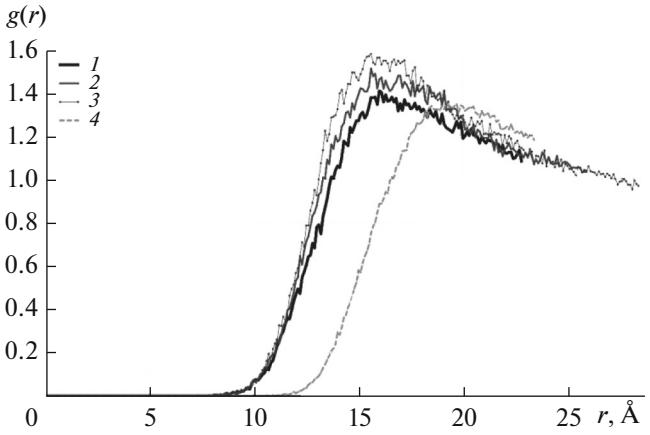

Fig. 3. The $g(r)$ RDFs of Na^+ ions relative to the CMs of the aggregates for systems containing (*1–3*) 16 and (*4*) 32 SDS molecules and (*1*, *4*) 3200, (*2*) 4800, and (*3*) 6400 water molecules and (*4*) 16 $CaCl_2$ molecules.

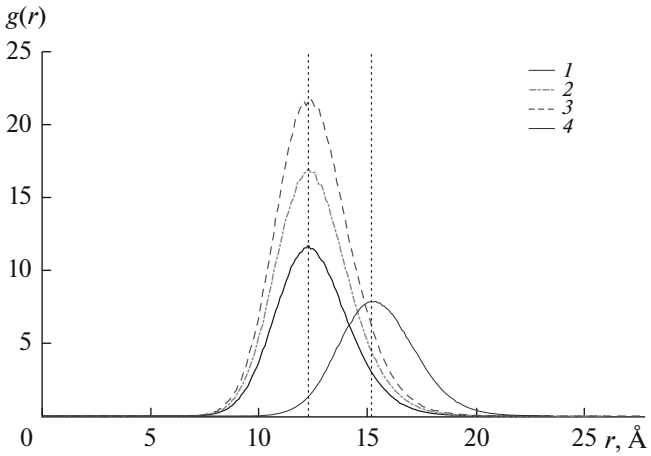

Fig. 4. The $g(r)$ RDFs of sulfur atoms relative to the CMs of the aggregates. The systems and denotations are the same as in Fig. 3.

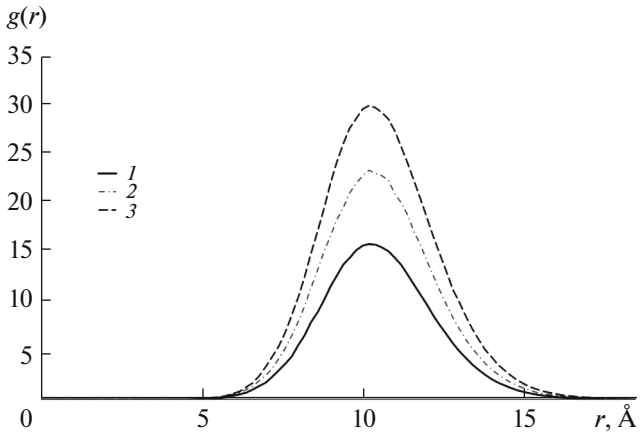

Fig. 5. The $g(r)$ RDFs of C_1 carbon atoms (closest to the polar head of a surface-active anion) relative to the CMs of the aggregates for systems containing 16 SDS molecules and (*1*) 3200, (*2*) 4800, and (*3*) 6400 water molecules.

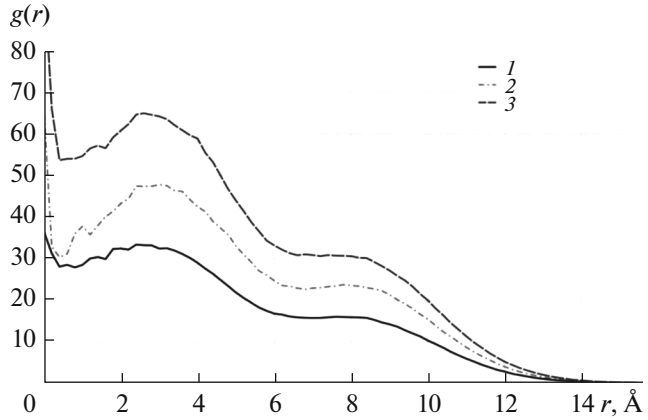

Fig. 6. The $g(r)$ RDFs of C_{12} carbon atom relative to the CMs of the aggregates. The systems and denotations are the same as those in Fig. 5.

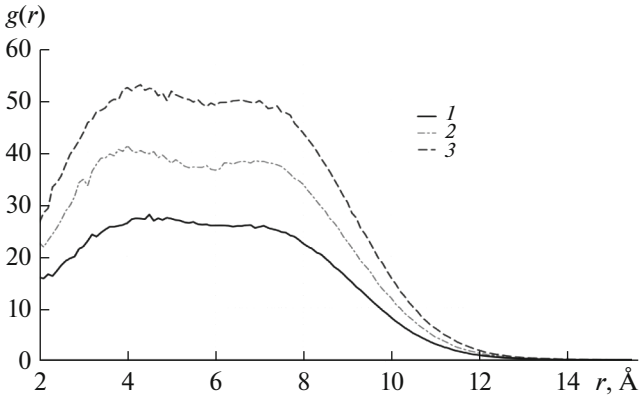

Fig. 7. The $g(r)$ RDFs relative to the CMs of the aggregates for C_7 carbon atom. The systems and denotations are the same as those in Fig. 5.

For the cases of 4800 and 6400 water molecules contained in the simulation cell, the RDF values at large r values approach unity, thereby indicating that the cell size is sufficient for monitoring the characteristic distribution of counterions. In Fig. 3, the RDFs of sodium ions begin to differ from zero at distances of nearly 7.8, 7.3, and 8.3 Å for the salt-free systems and at 10.2 Å in the presence of $CaCl_2$. Let us note, that these distances are markedly smaller than R_S. The analysis of the instantaneous system configurations with the use of the VMD software [29] has not shown counterions that penetrated the aggregate core. Thus, the rather small distance from some counterions to the aggregate CM indicates that they approach the CM when the aggregate shape changes, e.g., when the aggregate becomes more extended.

Figures 5–7 show the $g(r)$ RDFs of carbon atoms numbered according to their positions in the SDS molecule for systems containing 16 SDS molecules and 3200, 4800, and 6400 water molecules. It can be seen that the RDF of the carbon atom with serial number 1 (C_1 atom closest to the polar group of the surface-active ion) relative to the aggregate CM has the only distinctly pronounced maximum at all considered surfactant concentrations (see Fig. 5). The position of the maximum along the r axis is almost the same and amounts to nearly 10.5 Å for all considered concentrations. At the same time, analogous RDF curves for the carbon atom with serial number 7 (the seventh C_7 atom from the head of the surface-active ion) (Fig. 7) exhibits two local maxima (or a maximum and a plateau) at $r \approx 4.0$–4.5 and 7 Å at all considered surfactant concentrations. An analogous figure for the carbon atom with serial number 12 located at the end

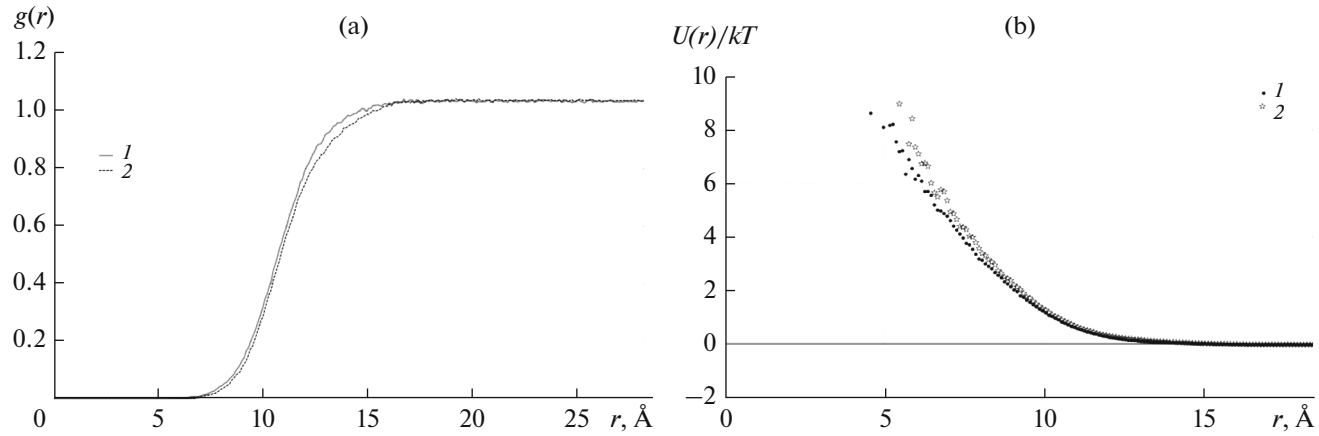

Fig. 8. Panel (a): the $g(r)$ RDFs relative to the aggregate CM for (*1*) H and (*2*) O atoms of H_2O molecules for the system containing 16 SDS and 6400 H_2O molecules and panel (b): the $U(r)$ potentials of mean force applied to (*1*) H and (*2*) O atoms of water molecules as functions of distance r from the aggregate CM for the system containing 16 SDS and 6400 H_2O molecules.

of the hydrocarbon tail in SDS shows distinct maxima at $r = 0$ (aggregate CM) and at $r \approx 3$ Å (Fig. 6). Weak local maxima or plateaus are observed at $r \approx 7$–8.5 Å. The observed double and triple maxima and plateaus seem to exist only for small premicellar aggregates and are not inherent in large stable SDS micelles, in which hydrocarbon radicals of surface-active ions must be almost ultimately unfolded.

The $g(r)$ RDFs for oxygen and hydrogen atoms of water molecules relative to aggregate's CM are presented in Fig. 8a for system containing 6400 H_2O and 16 SDS molecules. Note that oxygen and, especially, hydrogen atoms of water molecules may approach the aggregate CM at a distance shorter than that for sodium ions (see Fig. 3). The RDFs of hydrogen and oxygen atoms have no local maxima near the aggregate surface (Fig 8a). Figure 8b shows the $U(r) = -\ln(g(r))$ potentials (expressed in thermal units kT, where k is the Boltzmann constant) of mean force applied to oxygen and hydrogen atoms of water molecules as functions of distance r from the aggregate CM.

Figure 9 presents the RDFs of oxygen atoms of water molecules relative to different atoms of an SDS aggregate with an aggregation number of 16. It can be seen that the RDFs of the oxygen atoms of water molecules relative to sulfur and oxygen atoms belonging to the aggregate have pronounced high peaks at small r values. These data lead us to conclude that the polar head groups of surface-active ions attract water molecules or, in other words, are wetted with water. At the same time, the RDFs of oxygen atoms belonging to water molecules relative to C_1, C_7, and C_{12} carbon atoms (located near the head of the surface-active ion and in the middle and at the end of the tail) have a pattern that is, most probably, characteristic to nonwetting. Because of the small aggregation number of the considered aggregate, the hydrocarbon groups may occupy a substantial part of its surface (see Fig. 10); therefore, part of the aggregate surface appears to be nonwettable. Hence, the surface of an SDS aggregate with an aggregation number of 16 appears to contain both wettable and nonwettable regions; i.e., it turns out to be partly wettable. At the same time, the RDFs of water molecule atoms relative to the center mass of an aggregate with an aggregation number $n = 16$, that exhibit no peaks near the aggregate surface (see Fig. 8a), suggest that the nonwettable regions of the surface play a greater role in the interaction between this aggregate and water molecules than wettable regions do. In other words, the effective force of the interaction between the small aggregate under consideration and water molecules corresponds to its incomplete wetting (see Fig. 8b).

The $g(r)$ RDFs of Ca^{2+}, Cl^-, and Na^+ ions and S atoms relative to the aggregate CM for a system containing 32 SDS, 3200 H_2O, and 16 $CaCl_2$ molecules are presented in Fig. 11. It can be seen that the cations are located closer to the aggregate's CM than the anions due to the electrostatic attraction to the negatively charged aggregate surface.

To study the aggregation kinetics with the use of molecular dynamics trajectories, a reliable algorithm is needed for the automatic determination of aggregation numbers and of the number of aggregates in a micellar solution. Therefore, a criterion showing that two surface-active ions belong to the same aggregate must, primarily, be established. When such a criterion has been determined, the number of aggregates in a simulation cell and their aggregation numbers may be found recursively. For example, let three surface-active ions, A, B, and C, be located in the cell. Initially, we use the selected criterion to verify whether A and B ions belong to the same aggregate. Let us assume that the criterion has been met and ions A and B belong to the same aggregate. In this case, ion C will

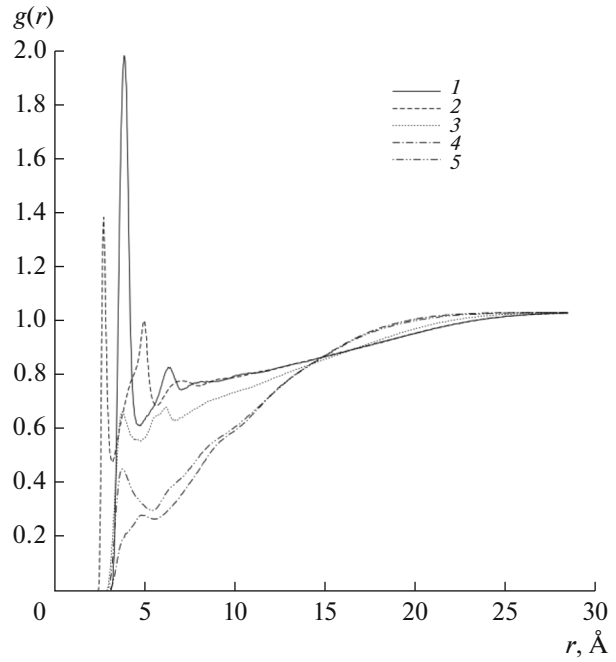

Fig. 9. The RDFs of O atoms belonging to H_2O molecules relative to (*1*) S, (*2*) OS, (*3*) C_1, (*4*) C_7, and (*5*) C_{12} atoms of surface-active ions for a system containing 16 SDS and 6400 H_2O molecules.

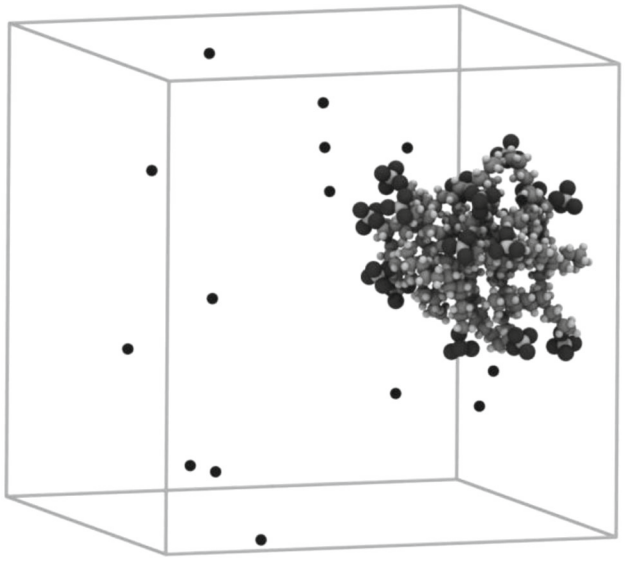

Fig. 10. The snapshot of a system containing 16 SDS and 6400 water molecules.

belong to the same aggregate, provided that the selected criterion is met for, at least, one of the A and C or B and C pairs. This algorithm may be easily generalized to an arbitrary number of surface-active ions in the cell.

In an aqueous SDS solution, surface-active ions are assembled into aggregates due to the hydrophobic effect, with some fragments of hydrocarbon tails of different surface-active ions appearing to be located close to each other. We suppose that two surface-active ions belong to the same aggregate, provided that the minimum distance between any carbon atoms belonging to different surface-active ions is smaller than some (preset in advance) value R_{min}. The R_{min} value is selected empirically. If the only aggregate is visually observed in a system for a long time, we select the maximum value of R_{min} at which all surface-active ions in the system belong to the same aggregate. For example, the same value R_{min} = 5.521 Å has been selected for the considered systems containing 16 SDS molecules and different numbers of water molecules (3200, 4800, and 6400). Then, the obtained R_{min} value may be used for the automatic analysis of more complex cases, in which a system contains several aggregates.

The results of using the described above algorithm for determining numbers of aggregates N_{agg} in different systems are illustrated in Fig. 12. Three systems containing 16 SDS molecules and different numbers of water molecules (3200, 4800, and 6400) have been considered. The reliability of the algorithm operation has been increased by averaging the instantaneous numbers of aggregates over time periods of 200 ps. It can be seen that, at the initial stage of relaxation (for a few first nanoseconds after the onset of simulation), the number of aggregates rapidly decreases in each system. During a time interval from 3 to 9 ns, each system contains two to four aggregates. Finally, a single aggregate with aggregation number $n = 16$ is formed in the cell within 10–30 ns after the onset of simulation (depending on the overall surfactant concentration). The aggregation of all surface-active ions in the cell has occurred most rapidly in the system containing 6400 water molecules (the lowest surfactant concen-

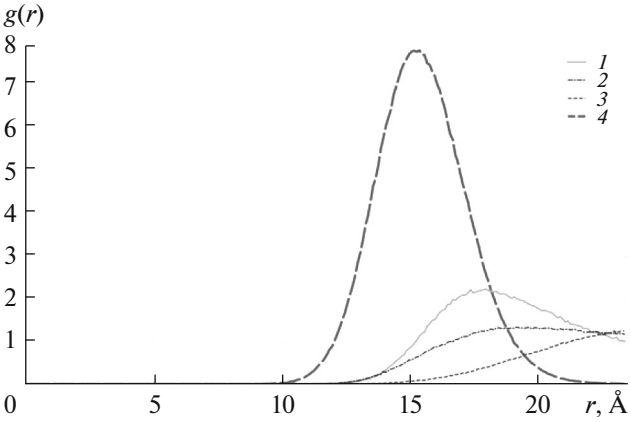

Fig. 11. The $g(r)$ RDFs relative to the aggregate's CM for (*1*) Ca^{2+}, (*2*) Na^+, and (*3*) Cl^- ions and (*4*) S atoms for the system containing 32 SDS, 16 $CaCl_2$, and 3200 H_2O molecules.

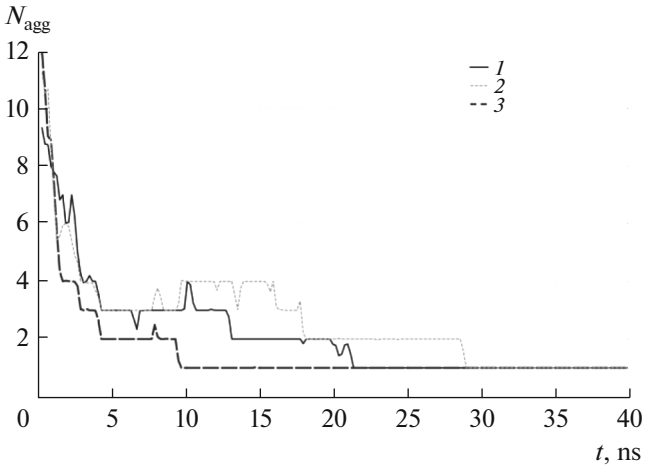

Fig. 12. Dependences of number of aggregates N_{agg} on simulation time t. The systems and denotations are the same as those in Fig. 5.

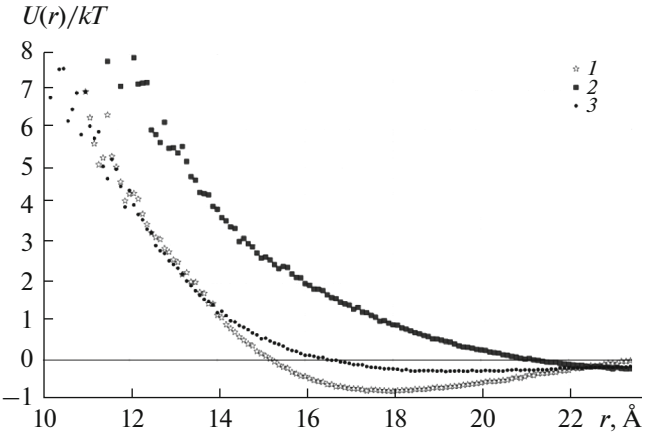

Fig. 13. The $U(r)$ potentials of mean force applied to (*1*) Ca^{2+}, (*2*) Cl^{-}, and (*3*) Na^{+} ions as functions of distance r from the aggregate CM for a system containing 32 SDS, 3200 H_2O molecules, and 16 $CaCl_2$ molecules.

tration). The formation of a single aggregate in the system with 3200 water molecules (the highest surfactant concentration) took more time. The single aggregate in the system with 4800 water molecules (the intermediate surfactant concentration) was the last to be formed. Unfortunately, we are not able to infer more essential conclusions on the aggregation kinetics in the studied systems because of the limitations imposed on the system sizes and the time of process monitoring. For proper studying the aggregation kinetics, it is necessary to consider larger systems during longer times. Moreover, the determination of the aggregation rate of surface-active ions depending on surfactant concentration requires performing numerous tests for each concentration under different initial conditions followed by data averaging.

For a system containing 32 SDS, 3200 H_2O and 16 $CaCl_2$ molecules, dimensionless potentials of mean force $U(r) = -\ln(g(r))$ were calculated using the $g(r)$ RDFs presented in Fig. 11 for calcium, chlorine, and sodium ions. Corresponding dependences of the potential of mean force on r are presented in Fig. 13. The plots show that chlorine ions are repulsed from the aggregate (the r derivative of the potential does not reverse its sign throughout the r range; i.e., the direction of the force remains unchanged), while sodium and calcium ions are repulsed at small distances from the aggregate due to the effect of an excluded volume; however, being distanced from the aggregate CM, they begin to be attracted to the aggregate due to the Coulomb interactions. Therewith, the depth of the potential well in the curve for the calcium ion–aggregate interaction is of the order of kT; i.e., divalent calcium ions appear to be strongly bonded to the aggregate, while there is no strong binding between the aggregate and monovalent sodium counterions (the potential well is too shallow).

CONCLUSIONS

The work presents the results of all-atom molecular dynamics simulation of aqueous dodecyl sodium sulfate solutions (salt-free solutions and those containing additives of $CaCl_2$). All atoms of both the solvent and surfactant were explicitly taken into account in the simulation and carried partial charges. The electrostatic interactions in the system were treated by the Ewald method. During the simulations we observed the self-assembly of the SDS surface-active ions into the premicellar aggregates. The obtained molecular dynamics trajectories were used to study the structural properties of micellar SDS solutions with different concentrations and SDS solutions containing the 2 : 1 electrolyte admixture. The aggregation kinetics of surface-active ions was studied in the salt-free solutions at short times. The effective radii of premicellar surfactant aggregates were found, and the RDFs of different ions and atoms relative the centers of mass of the aggregates were obtained.

The plots of the RDFs for sodium ions and sulfur atoms, as well as the values of the effective radii of the aggregates, suggest that the size of a premicellar aggregate in the cell with a preset number of surfactant molecules virtually does not depend on surfactant concentration in the considered concentration range. In addition, these plots show that some counterions appear to be at a rather small distances from the aggregate CM; however, they do not penetrate the aggregate core. Therefore, it may be inferred that the aggregate shape varies in the course of simulation; i.e., it becomes sometimes almost spherical, sometimes more extended.

The aggregation rate in the simulation cell was monitored. At an initial stage of relaxation (within a few nanoseconds after the onset of the simulation), the number of aggregates decreased rather rapidly and a single aggregate was formed in 10–30 ns.

The RDFs obtained for hydrogen and oxygen atoms of water molecules had no local maxima near the aggregate surface. Hence, one may conclude that the aggregate surface was partly wetted with water.

The RDFs of carbon atoms relative to the CM of a premicellar aggregate with aggregation number $n = 16$ show one, two or three maxima depending on the position of a carbon atom in the hydrocarbon radical of a surface-active ion and on the surfactant concentration in the simulation cell.

The plot of the potential of mean force of the interaction of sodium and calcium ions with a premicellar SDS aggregate with aggregation number $n = 32$ indicates that only calcium ions appear to be strongly bonded to this aggregate.

ACKNOWLEDGMENTS

The study was performed using the computational resources provided by Resource Center "Computer Center of SPbU" (http://www.cc.spbu.ru/). The work was supported by the Russian Science Foundation, project no. 14-13-00112.

REFERENCES

1. Babintsev, I.A., Adzhemyan, L.Ts., and Shchekin, A.K., *J. Chem. Phys.*, 2012, vol. 137, p. 044902.
2. Babintsev, I.A., Adzhemyan, L.Ts., and Shchekin, A.K., *Soft Matter*, 2014, vol. 10, p. 2619.
3. Babintsev, I.A., Adzhemyan, L.Ts., and Shchekin, A.K., *J. Chem. Phys.*, 2014, vol. 141, p. 064901.
4. Shchekin, A.K., Babintsev, I.A., Adzhemyan, L.Ts., and Volkov, N.A., *RSC Adv.*, 2014, vol. 4, p. 51722.
5. Shchekin, A.K., Kshevetskiy, M.S., and Pelevina, O.S., *Colloid J.*, 2011, vol. 73, p. 406.
6. Zakharov, A.I., Adzhemyan, L.Ts., and Shchekin, A.K., *J. Chem. Phys.*, 2015, vol. 143, p. 124902.
7. Mohan, G. and Kopelevich, D.I., *J. Chem. Phys.*, 2008, vol. 128, p. 044905.
8. Shelley, J.C. and Shelley, M.Y., *Curr. Opin. Colloid Interface Sci.*, 2000, vol. 5, p. 101.
9. Brodskaya, E.N., *Colloid J.*, 2012, vol. 74, p. 154.
10. Ladanyi, B.M., *Curr. Opin. Colloid Interface Sci.*, 2013, vol. 18, p. 15.
11. Volkov, N.A., Divinskiy, B.B., Vorontsov-Velyaminov, P.N., and Shchekin, A.K., *Colloids Surf. A*, 2015, vol. 480, p. 165.
12. Volkov, N.A., Tuzov, N.V., and Shchekin, A.K., *Fluid Phase Equilib.*, 2016, vol. 424, p. 114.
13. Sammalkorpi, M., Karttunen, M., and Haataja, M., *J. Phys. Chem. B*, 2007, vol. 111, p. 11722.
14. Sammalkorpi, M., Karttunen, M., and Haataja, M., *J. Phys. Chem. B*, 2009, vol. 113, p. 5863.
15. Kawada, S., Komori, M., Fujimoto, K., Yoshii, N., and Okazaki, S., *Chem. Phys. Lett.*, 2016, vol. 646, p. 36.
16. Lyubartsev, A.P. and Laaksonen, A., *Comput. Phys. Commun.*, 2000, vol. 128, p. 565.
17. Klaud, J.B., Venable, R.M., Freites, J.A., O'Connor, J.W., Tobias, D.J., Mondragon-Ramirez, C., Vorobyov, I., Mackerell, A.D., and Pastor, R.W., *J. Phys. Chem. B*, 2010, vol. 114, p. 7830.
18. http://mackerell.umaryland.edu/charmm_ff.shtml.
19. Lennard-Jones, J.E., *Proc. R. Soc. London A*, 1924, vol. 106, p. 463.
20. Beglov, D. and Roux, B., *J. Chem. Phys.*, 1994, vol. 100, p. 9050.
21. Brooks, B.R., Bruccoleri, R.E., Olafson, B.D., States, D.J., Swaminathan, S., and Karplus, M., *J. Comput. Chem.*, 1983, vol. 4, p. 187.
22. Durell, S.R., Brooks, B.R., and Ben-Naim, A., *J. Phys. Chem.*, 1994, vol. 98, p. 2198.
23. Neria, E., Fischer, S., and Karplus, M., *J. Chem. Phys.*, 1996, vol. 1902.
24. Jorgensen, W.L., Chandrasekhar, J., Madura, J.D., Impey, R.W., and Klein, M.L., *J. Chem. Phys.*, 1983, vol. 79, p. 926.
25. Tuckerman, M., Berne, B.J., and Martyna, G.J., *J. Chem. Phys.,* 1992, vol. 97, p. 1990.
26. Ewald, P., *Ann. Phys.* (New York), 1921, vol. 369, p. 253.
27. Lyubartsev A., MDynaMix Package version 5.2.7 User manual, Division of Physical Chemistry, Stockholm University, 12 January 2015.
28. Bogusz, S., Venable, R.M., and Pastor, R.W., *J. Phys. Chem. B*, 2000, vol. 104, p. 5462.
29. Humphrey, W., Dalke, A., and Schulten, K., *J. Mol. Graph.*, 1996, vol. 14, p. 33.

Translated by A. Kirilin